
Article:
Aboalhamayie, A. orcid.org/0000-0002-3934-5976, Zhang, Y. and Ghamari, M. (2025) Iron particle in liquid fuel combustion technology for nonoxidative storage and easy burning. Fuel, 380. 133240. ISSN: 0016-2361

https://doi.org/10.1016/j.fuel.2024.133240

Iron Particle in Liquid Fuel Combustion Technology for Nonoxidative Storage and Easy Burning

Ahmed Aboalhamayie[a], Yang Zhang[a,1], Mohsen Ghamari[b]

[a] *Department of Mechanical Engineering, The University of Sheffield, Sheffield S1 3JD, United Kingdom*

[b] *Department of Mechanical and Electrical Engineering, Wilkes University, Wilkes-Barre, PA 18766, USA*

Abstract

This study investigates an iron particle in liquid fuel combustion technology with liquid fuel as an anti-oxidization agent for the iron fuel particles, which has the advantage of easy combustion and nonoxidative iron particle storage. These slurry like iron particles in liquid fuel can be ideal for furnaces and boilers. Micron and nano-sized iron particles, concentrated at a 30% mass fraction, demonstrate enhanced reductions in total combustion time and increased micro-explosion intensity. The study observes that suspensions of micron-sized particles progress through preheating, ignition, stable combustion, and intense micro-explosion. In contrast, a dense colloidal suspension of iron nanoparticles in diesel fuel undergoes preheating, classical combustion, bubble growth with low-intensity secondary atomization, and the combustion of agglomerated nanoparticles, resulting in a glowing solid residue. A hybrid dense colloidal formulation incorporating micron and nano suspensions at a combined mass fraction of 30% was

[1] *Corresponding Author*. The University of Sheffield, Department of Mechanical Engineering, Sir Frederick Mappin Building, Sheffield S1 3JD, United Kingdom. E-mail address: yz100@sheffield.ac.uk

introduced to prevent particle agglomeration and achieve faster micro-explosions. This formulation leads to a significant 83% reduction in total combustion time. The distinctive behavior is attributed to iron nanoparticles' higher specific surface area, leveraging diesel's nucleation and bubble growth for mid-intensity puffing within the droplet. Nucleation metastability intensifies superheating values, leading to internal pressure in the bubble grown via homogeneous nucleation and culminating in intense puffing, followed by a micro-explosion. This cascade effect highlights the potential of iron particles as a clean source with high energy density, providing novel insights for practical industrial applications. The observed micro-explosion intensity underscores the promise of this innovative approach, paving the way for advancements in cleaner and more efficient iron particle slurry combustion technology.

Keywords: Droplet Combustion; Iron Particles in Liquid Fuel; Total Combustion Time; Micro-explosion; Nonoxidative Storage

1. Introduction

The urgent transition from overreliance on fossil fuels to sustainable, renewable energy sources is a pivotal challenge in advancing new fuel and combustion technologies. Recent research has highlighted metallic elements, particularly iron and boron, as potential candidates for green power generation [1–3]. Among these, iron has been identified as a leading contender, with micron-sized iron powder proposed as an innovative renewable energy carrier [4]. Significant efforts have been directed toward studying nano and micron-sized iron particles (under 10 μm) for power generation applications, with the goal of reducing emissions and enhancing industrial energy efficiency [5,6]. Research into the combustion and ignition characteristics of single iron particles has expanded our understanding of these processes, utilizing various experimental approaches. For example, Shuai Zhang et al. [7] determined that calcination temperature is the most influential factor affecting the reactivity of natural iron ore in chemical looping combustion, with optimal conditions identified as a 15 °C/min heating rate, 1050 °C temperature, and 60 minutes of calcination for stable performance. Meanwhile, Li et al. [8] established that particle size plays a crucial role in determining ignition delay, burning time, and total combustion duration, particularly for particles exceeding 40 μm, independent of oxygen concentration. Furthermore, Yuan Yao et al. [9] explored powdered iron combustion as a circular energy carrier, observing spectral emissivities between 0.18 and 0.46 and temperatures ranging from 2300 K to 2800 K, influenced by oxygen concentration and particle density. Ning et al. [10] introduced refined techniques for analyzing single metal particle combustion, emphasizing a two-stage combustion process that is sensitive to oxygen levels and providing detailed burn time measurements for iron particles. Additionally, Pál Tóth et al. [11] revealed that pulverized sponge iron (PSI), combusted in a McKenna flat flame

burner, primarily undergoes heterogeneous combustion, forming solid oxides and an unexpected microflame on the particle surface, with high-magnification shadowgraphy capturing near-instantaneous melting. In another study, Junlei Sun et al. [12] employed ReaxFF molecular dynamics simulations to investigate the thermal properties of bulk iron and Fe nanoparticles, concluding that while defects (0%-10%) in nanoparticles raise system energy near melting points, they do not alter the melting temperature. Recent studies focusing on micrometric iron particle combustion (38–53 μm) under varying oxygen levels found that while particle size minimally impacts peak temperature, it significantly influences burnout duration, with oxygen concentration notably affecting both peak temperature and burnout time, especially beyond 50% oxygen concentration [13]. Moreover, WANG Jin-yun et al. [14] underscored the substantial energy density and future potential of nano iron powder as a transportation fuel, achieving a specific impulse of 3500 N•s/kg. Although the combustion of solid iron particles is relatively straightforward, long-term storage poses a challenge due to the oxidation susceptibility of iron, particularly in the presence of moisture. For nano iron particles, their reactivity in the atmosphere is significantly high. Even a slight increase in temperature or minimal friction can cause ignition. This highlights the need for an effective storage technique to prevent these particles from coming into direct contact with air. Hydrocarbon liquid fuels like diesel, with their hydrophobic and non-polar nature, could serve as an effective anti-oxidation medium, similar to how alkali metals such as potassium are stored in kerosene to prevent oxidation. Blending iron particles with liquid fuel may facilitate both easy combustion and non-oxidative storage. Experimental studies have shown that incorporating metallic particles as a colloidal suspension, with particle sizes ranging from nano to micro-scale, enhances combustion characteristics such as burning and evaporation rates, total combustion

time, micro-explosion intensity, and ignition delay. Adhes Gamayel et al. [15] reviewed advances in single droplet combustion for fuel characterization, emphasizing key experimental methods and proposing future research directions in this evolving field. A.M.-D. Faik et al. [16] utilized high-speed imaging to examine liquid-phase dynamics during multicomponent fuel droplet combustion, focusing on phenomena such as nucleation, bubble formation, and secondary atomization, and comparing the burning rates of parent droplets with their sub-droplets, noting significant combustion-induced changes in droplet geometry. Additionally, secondary nanoparticle contamination, such as from soot particles, has been found to impact burning characteristics [17,18]. Srinibas Karmakar et al. [19] demonstrated that nanofuel droplets containing amorphous boron exhibit smoother combustion with minor puffing and form porous shells, whereas crystalline boron leads to intense micro-explosions and dense, impermeable shells, with amorphous boron showing superior combustion performance. Aboalhamayie et al. [20] explored the impact of various carbon-based nanoparticles on the evaporation rate of jet fuel droplets. Gan et al. [21,22] conducted experimental studies on droplets containing nano and micron-sized aluminum particles, revealing nuanced, size-dependent burning behaviors influenced by surface functionalization and surfactants. Nano iron particles have also been observed to reduce soot and unburned hydrocarbon emissions in diesel engines [23]. Most previous research has primarily focused on the effects of micro and nano particles on liquid combustion at very low concentrations or on the combustion of single iron particles, rather than on the use of iron particles as a primary fuel at concentrations exceeding 25%. While high concentrations of iron particles could have detrimental effects in internal combustion engines due to their mechanical components, they should not pose a problem for combustion devices such as furnaces and boilers. A slurry of iron particles and liquid

fuels could be ideal for combustion and non-oxidative storage. Diesel fuel, primarily composed of aliphatic and aromatic hydrocarbons, acts as a non-polar and hydrophobic solvent, which prevents water absorption and engine complications while maintaining high-energy density, a crucial factor for various applications. This study aims to investigate the combustion mechanism of iron particles in liquid fuel combustion technology for devices such as furnaces and boilers, leveraging their potential for long-term non-oxidative iron particle storage. Addressing the oxidation susceptibility of iron particles is critical to establishing them as a viable carbon-free fuel source, a concern that has received minimal attention in the combustion community. In this investigation, the combustion of high-concentration colloidal suspensions of micro and nano-sized iron particles in diesel fuel was experimentally studied. A novel hybrid mixture of equal amounts of micron-sized and nano-sized iron particles was developed, demonstrating a significantly reduced combustion time and higher micro-explosion intensity. Aside from providing a medium to incorporate iron combustion into existing systems, diesel fuel can prevent the oxidation of iron particles during long-term storage. The deployment of suspended droplets onto a SiC fiber, facilitated by a meticulously designed apparatus with high-speed photography and backlighting, provided comprehensive insights into combustion dynamics, examining key parameters such as burning rate, total combustion time, micro-explosion phenomena, and underlying mechanisms.

2. Materials and sample preparation technique

The current study centers around two distinct types of iron particles: 40 nm particles, denoted as Fe-nm (Nanostructured and Amorphous Materials Inc., Product ID 0262HW), and 10 micro-scale particles, denoted as Fe-μm (Merck Life Science UK Limited, Product ID 1038190500), as shown in Figure 1. The physical characteristics

of each particle are also summarized in Table 1. Small scale iron particles are highly reactive in air and should be handled carefully. As such, the principal objective of this research is to use diesel fuel as a non-oxidative storage environment for iron particles and to assess the influence of this encapsulation on the droplet combustion characteristics.

Table 1. Physical properties of iron particles.

Particle Type	Fe-µm	Fe-nm
Size (µm & nm)	10	40
True Density (g/cm^3)	7.86	7.86
Purity%	99.9	99.9
Color	Gray	Black

To prepare fuel samples, iron particles were weighed and manually mixed in the base fuel. It is worth mentioning that the use of a magnetic mixer was avoided as the magnetic field generated by the mixer will aggregate particles around its magnetized regions. Contrary to the normal practice in preparing colloidal suspension, using surfactant was omitted from this protocol. The rationale behind this decision stemmed from the realization that surfactants introduce effects divergent from combustion dynamics. It is worth highlighting that the presence of excessive surfactant induces the formation of undesirable macromolecules, characterized by long-chain molecular structures, in the solution, a phenomenon recognized as depletion stabilization [22,24]. To disperse particles in the base fuel, the mixture was treated in a sonication bath for a duration of 45 minutes. The stability of prepared samples was checked visually and it was determined that suspensions of Fe-nm, Fe-µm, and hybrid particles are stable for

20, 3, and 5 minutes after sonication, respectively. As such, the samples always remained in the sonication bath until seconds before conducting each experiment.

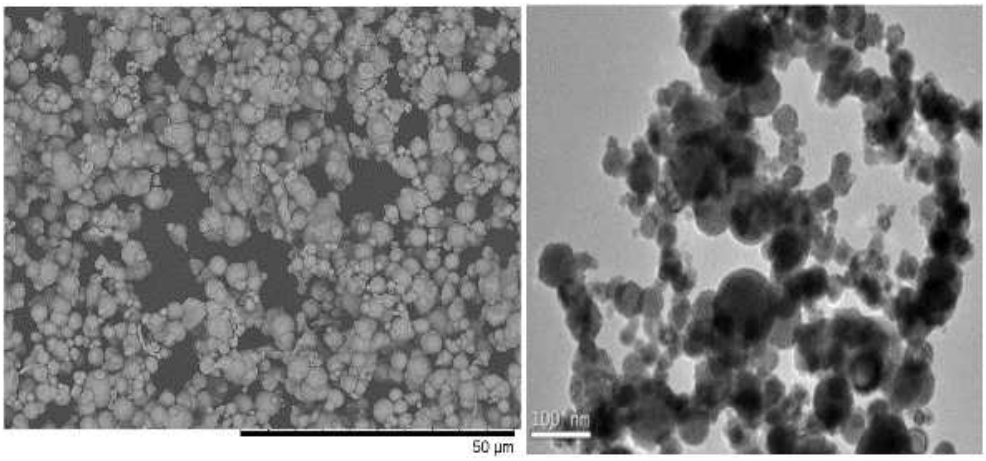

Fig. 1. SEM images of 10 µm iron particle (left) and 40 nm iron particles (right) [25]

3. Experimental methodology

The experimental apparatus was meticulously engineered to investigate the combustion behavior and the effects of morphological characteristics of iron particles. The system comprised several key components: a 3D-printed fiber support holder, a custom-designed heating element, a robotic arm gripper, a power supply, a backlighting system, a linear actuator for precise linear motion, and an integrated electronic circuit for system control. As illustrated in Figure 2, the experimental framework was designed to generate fuel droplets using a microsyringe, which were then deposited on a 100-micrometer SiC fiber. The fiber support holder, securely fixed and connected to the first linear actuator, was integrated with a pulse-width modulation (PWM) unit, enabling precise positioning of the heating element beneath the droplet and ensuring optimal alignment for high-speed camera capture. Furthermore, a second linear actuator was centrally positioned on the 3D-printed base frame, also controlled by a PWM module, to facilitate accurate positive and negative horizontal movements. An articulated

robotic gripper arm, equipped with a high-precision servo motor, was mounted atop the linear motion generator. This gripper arm featured a gripping mechanism with a divergence of 45 degrees and a convergence of -45 degrees, specifically designed to accommodate the heating elements. The heating elements were composed of a resistance wire, a ceramic insulator, a terminal block, and a 3D-printed support holder, as depicted in Figure 2(B). A bespoke heating element was strategically incorporated into the system and interfaced with an electronic circuit, playing a crucial role in providing precise temporal control of heating intervals and the corresponding energy input necessary to ignite the droplet. The heating element wire had a nominal diameter of 0.127 mm and an extended length of 40.15 mm, with an arched roller configuration featuring a 4 mm diameter. The ignitor heating element, shaped into a circular loop, emitting a striking red glow when activated. To capture the dynamic combustion process, a high-speed camera (Photron-SA4) was seamlessly integrated into the system, operating at a frame rate of 2000 frames per second, supported by electronic circuitry and a specialized backlighting system The camera was equipped with a Laowa 100mm f2.8 2X Ultra Macro lens to enhance clarity and resolution. A critical aspect of the experimental design was the precise manipulation of the distance between the droplet and the heating elements, which was adjusted in 2 to 3 mm intervals depending on the combustion response, as shown in Figure 2(A)(1). The synchronized system initiated the heating process by triggering the high-speed camera and activating the heating element to ignite the droplet, as depicted in Figure 2(B)(2). After 500 ms, the custom-designed heating element, attached to the robotic arm, diverged at -45 degrees, as represented in Figure 2(B)(3). The recording process then ceased, and the system returned to its original position, ready for subsequent experiments. Image processing and analysis were conducted using NASA Spotlight [26, 27] to eliminate any

interference from the fiber within the field of view, ensuring precise and clear documentation of the combustion events. The novelty of this system lies in its ability to precisely control and capture the combustion dynamics of fuel droplets.

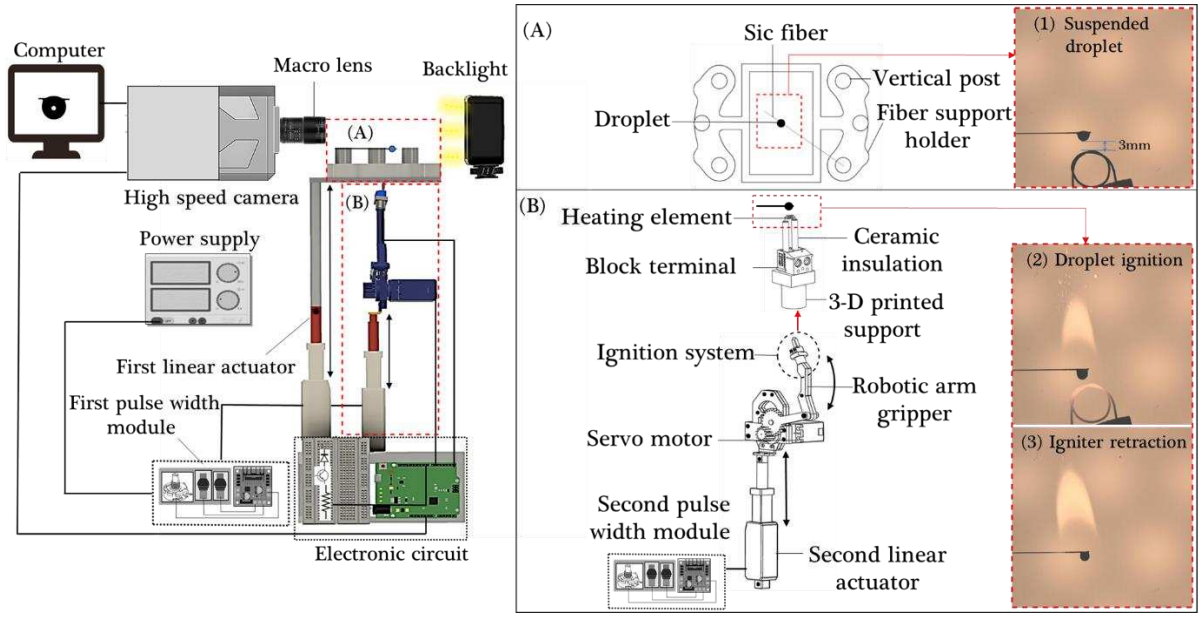

Fig. 2. Experimental setup for dense droplet combustion; (A) Fiber support holder configuration (B) Heating custom design and controlled system mobility

4. Results

The burning rate of a droplet can be evaluated using the classical d^2-law of droplet combustion as expressed by Equation (1). Here, d, d_0, t, and k are instantaneous and initial droplet diameters, time, and droplet combustion rate, respectively. In order to determine the burning rate from the experimental data, the time variation of the squared diameter during combustion was plotted against time, as shown in Figure 3, and the slope of the resulting diagram was considered as the burning rate.

$$\left(\frac{d}{d_0}\right)^2 = 1 - k\left(\frac{t}{d_0^2}\right) \qquad (1)$$

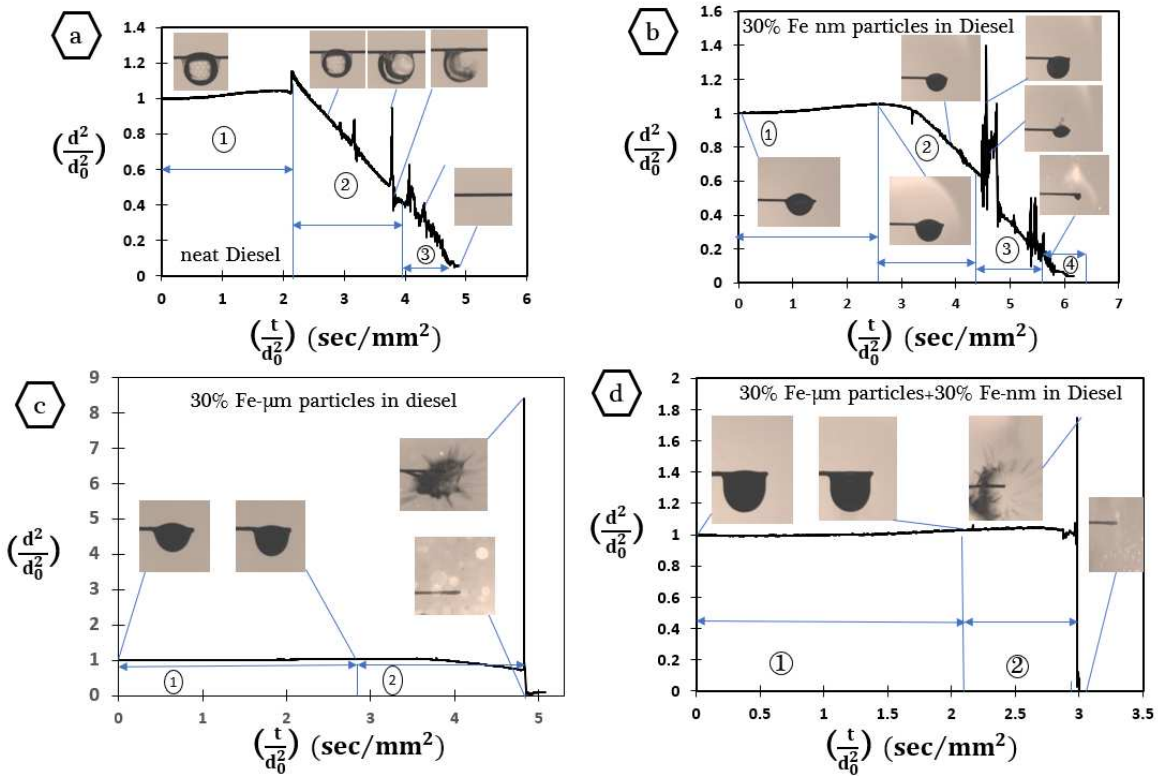

Fig. 3. Evolution of normalized droplet diameter square for a) neat diesel fuel; b) 30% Fe-nm particles in diesel fuel; c) 30% Fe-µm particles in diesel; d) 30% hybrid (equal amounts of Fe-µm and Fe-nm) in diesel fuel.

Figure 3 illustrates the evolution of squared diameter in four different cases, including (a) neat diesel fuel, (b) 30% (by weight) Fe-nm in diesel fuel, (c) 30% Fe-µm, and (d) 30% of hybrid particles (equal amount of both Fe-nm and Fe-µm) in diesel fuel. For each case, up to four stages with distinct characteristics were observed and identified in the diagrams shown in Figure 1.

In the case of neat diesel fuel (a), the combustion process initiates with preheating in Stage 1, followed by ignition. Stage 2 follows the classical d^2-law, during which an average burning rate of 0.34 mm^2/s was found. The heterogeneous nature of diesel fuel, with its diverse chemical substances and varying boiling points, leads to frequent nucleation, swelling, and puffing. Four discernible stages emerge upon adding 30% of Fe-nm particles to diesel fuel. Like neat diesel fuel, the process begins with pre-ignition heating, resulting in thermal expansion, as shown by Stage 1 in Figure 3b. Stage 2

begins with ignition and is followed by the d^2-law. Subsequently, combustion is accompanied by strong nucleation and swelling in Stage 3, followed by a micro-explosion leading to the burst of remaining liquid into the flame zone. Finally, in Stage 4, the solid combustion of Fe-nm particles left as a residue on the fiber was observed in a glow. The isolated residue combustion suggests a rate of particle agglomeration higher than that of droplet surface regression [28]. The average burning rate in Stages 2 and 3 was calculated to be 0.36 mm^2/s, showing a slight increase of only 3% compared to the neat diesel fuel. Previous studies, such as the works of Tanvir et al. [29, 30], have suggested that the nanoparticles can help in absorbing more radiation energy from the flame zone. In addition, such colloids typically have lower optical transmissivity than the base fuel. Higher radiation absorption, lower transmissivity, and enhanced energy transfer within the droplet due to enhanced thermal conductivity can lead to higher droplet evaporation and combustion. However, solid nanoparticles and their aggregates can also suppress the diffusion of more volatile species to the droplet surface, where evaporation and combustion occur. Therefore, at higher concentrations, such as the 30% particle loading in this study, the positive and negative effects cancel each other, leading to no significant enhancement in the burning rate.

Case (c), involving droplets of 30% Fe-µm in diesel fuel suspensions, shows only two stages and undergoes a shorter duration. Initially, the droplet goes through heating and thermal expansion, ending in ignition. However, the droplet lifetime after the ignition, is relatively short and ends with an intense micro-explosion generating very fine droplets. To examine the combustion characteristics of hybrid suspension in Case (d), equal amounts of 30% Fe-nm and 30% Fe-µm suspensions were mixed such that the prepared sample included 15% (by weight) of each particle type. Notably, the analysis showed two stages similar to those previously seen for suspension of Fe-µm, except

256 that the micro-explosion in Case (d) is stronger and occurs in a shorter period of time
257 after the ignition. The intense micro-explosion can be attributed solely to Fe-µm
258 particles, as it was not observed when only Fe-nm were added. This underscores the
259 hybrid addition of micronized materials as an effective strategy for expediting
260 combustion, enhancing the micro-explosion, and achieving a shorter combustion time.
261 Further elaboration on steady combustion values, combustion time, and micro-
262 explosion intensity will be presented in the subsequent section.

263 4.1. *Total time of combustion*

264 Figure 4 presents the average combustion time as a function of particle concentration.
265 In this study, combustion time is defined as the period between the appearance and
266 extinction of the flame in each experiment. Hence, the droplet burning time is
267 influenced by the combustion rate and the loss of mass during puffing and micro-
268 explosion events. The data in Figure 4 exhibits a significant drop in droplet burning
269 time as soon as iron particles, whether nano or micronized materials, are added. For the
270 colloids of Fe-nm, the 33% reduction can be attributed to increased burning rate and
271 mass loss during puffing events. On the other hand, the 58% and 83% reduction in
272 burning time for the colloids of Fe-µm and hybrid particles, respectively, can only be
273 considered to be due to mass loss as the combustion ends immediately after the micro-
274 explosion.

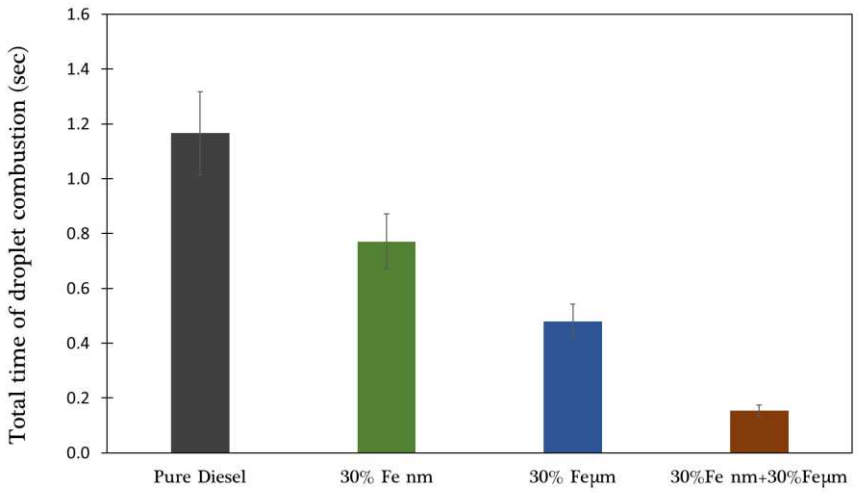

Fig. 4. Droplet burning time trends of different fuel droplets. Each data point indicates an average of five iterations. The error bars show the related standard deviation.

4.2. *Micro-explosion intensity and responsible mechanisms*

Micro-explosion intensity, as defined in previous studies, pertains to the frequency of multiple puffing events during the lifetime of the droplet. Accordingly, Singh et al. [31] characterized intensity as the frequency of the cycles defined by the rapid spikes and dips during puffing events, such as those seen in Stage 3 of Figure 3b. The micro-explosions observed in the combustion of Fe-μm and hybrid colloids include only one swelling event (spike) and end with the dissociation of the droplet into fine micro-droplets (i.e., no dips). Therefore, the intensity I is defined as the change in $(d/d_0)^2$ from the time swelling begins (point a) to the moment explosion occurs (point b), as shown in Figure 5 and expressed by Equation 2.

$$I = \frac{\left[\left(\frac{d}{d_0}\right)_b^2 - \left(\frac{d}{d_0}\right)_a^2\right]}{[t_b - t_a]} \qquad (2)$$

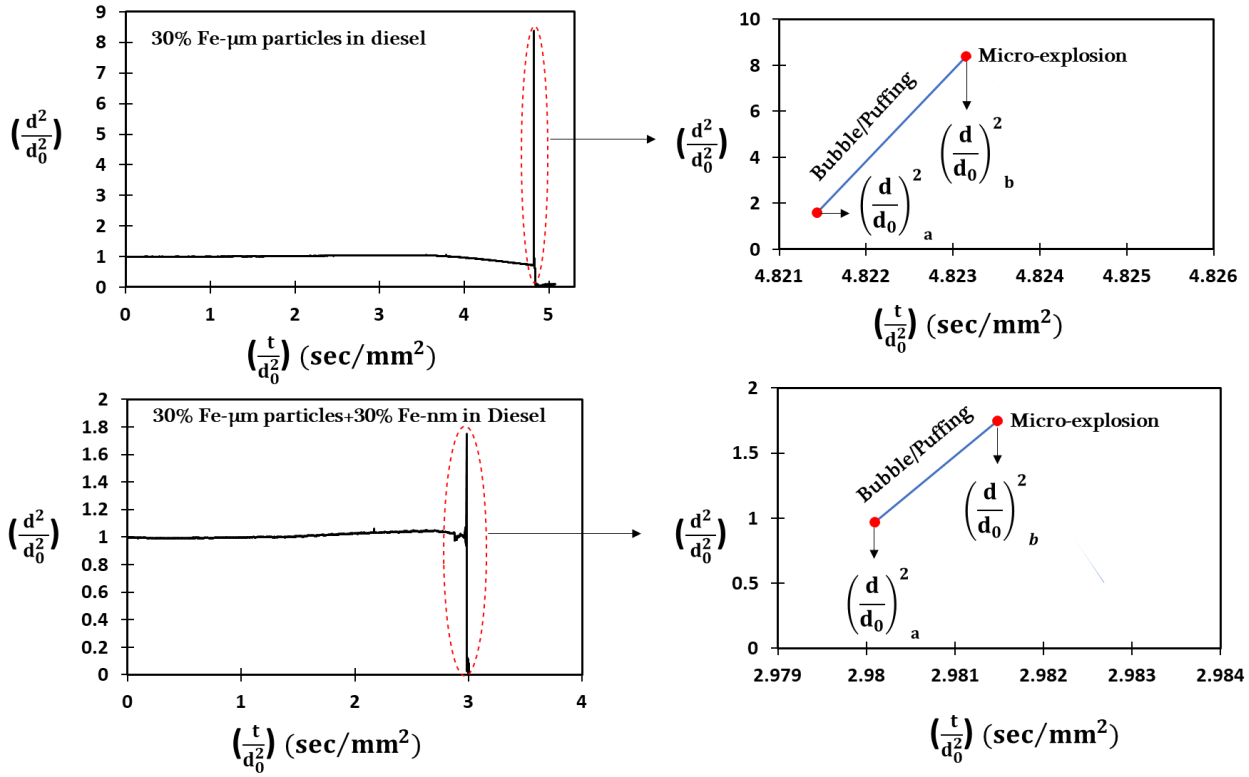

288

289 Fig. 5. Single micro-explosion events at the end of droplet combustion (Cases 3 and
290 4) represented by a magnified view of evolution of squared diameter ratio.

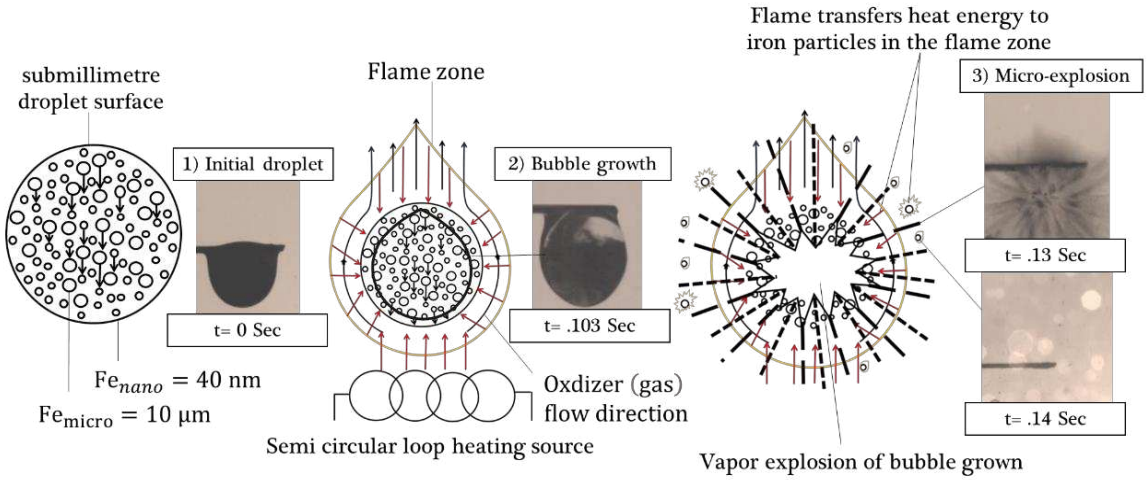

291

292 Fig. 6. Mechanism configuration represents the combustion process and intensity of
293 micro explosion occurrences in 30% hybrid Fe-µm and Fe-nm in diesel fuel

294 The average intensity of micro explosion based on a minimum of five experiments was
295 found to be 5300 sec^{-1} for colloids of 30% Fe-µm particles and 7300 sec^{-1} for colloids
296 of 30% hybrid particles. There is a multitude of mechanisms to explain micro-explosion
297 in multicomponent fuels. Still, the accumulation of particles near the surface in high

concentration colloids is believed to be the primary mechanism responsible for an intense micro-explosion as shown in Figure 6: Firstly, the accumulation of iron particles with less volatility and higher boiling points near the droplet surface instigates an elevation in the droplet temperature, effectively reaching a value beyond the boiling point of the base fuel. In contrast, the droplet core exhibits a heightened concentration of more volatile components characterized with lower boiling points. Consequently, the volatile constituents within the droplet interior have the potential to surpass local boiling points, resulting in the accumulation of a substantial degree of superheat. This phenomenon may culminate in the initiation of homogeneous nucleation, as represented by Figure 6-(2) and 6-(3), and characterized by an exceedingly rapid gasification rate, leading to an intense internal pressure surge and ultimately resulting in the catastrophic fragmentation of the droplet [32].

The particle accumulation also forms a porous shell that traps the more volatile base fuel. As the base fuel and fuel vapor travel to the droplet surface, they face resistance from the shell; hence, pressure builds up. Finally, the pressure reaches such high values that the shell cannot tolerate it, and therefore, a strong microexplosion happens. To better understand the mechanism responsible for different intensities of micro-explosion in Fe-μm and hybrid colloids, it is crucial to analyze the particle shell and their morphologies. To obtain samples of particle aggerates without combustion, the distance from the heating element to the droplet and its temperature was adjusted so that the droplet ran out of base fuel relatively quickly and without triggering any ignition. Finally, the residues that remained on the fiber were collected and studied using a Hitachi TM3030 Tabletop Scanning Electron Microscope, where the images are shown in Figures 7a to 7d. Figures 7a and 7b display Fe-μm agglomerate formed by a packed particle system. In a combustion case, the droplet surface regression from the

flame side and bubble formation from the droplet inside push the particles closer to the surface to form a porous shell. As the particles pack into each other, the shell becomes less permeable until it shatters due to the immense internal pressure. However, in the case of hybrid colloids where Fe-nm particles are present, a thinner shell of Fe-nm is formed on top of the inner Fe-µm. As was previously stated, nanosized particles are more effective in absorbing thermal radiation, and their presence near the droplet's surface leads to higher energy transfer to the droplet. The enhanced energy absorption can explain the shorter time between ignition and micro-explosion in hybrid colloids. In addition, Fe-nm particles can fill the void between the Fe-µm particles and form a sheet at the surface, making the shell even more impermeable than the shell formed in a Fe-µm colloid. Thus, a more intense micro-explosion follows. While the droplet surface regression and inner bubble growth are the dominating forces leading to the formation of a shell in colloids of microparticles, the random Brownian motion is primary transport mechanism responsible for particle aggregation when only nanoparticles are present [22]. Therefore, a more porous and homogeneous agglomerate is formed in Fe-nm colloids due to faster particle diffusion. The higher porosity level then allows the base fuel and fuel vapor to transport toward the surface, leading to several weak puffing events rather than an intense micro-explosion. Collecting post-combustion samples is challenging as the very strong microexplosion completely scatters particles. However, other studies such as the work of Baigmohammadi et al. [33] have suggested that Fe particles will convert into Fe oxide in a combusting environment but can be later reduced to Fe through a series of recycling processes.

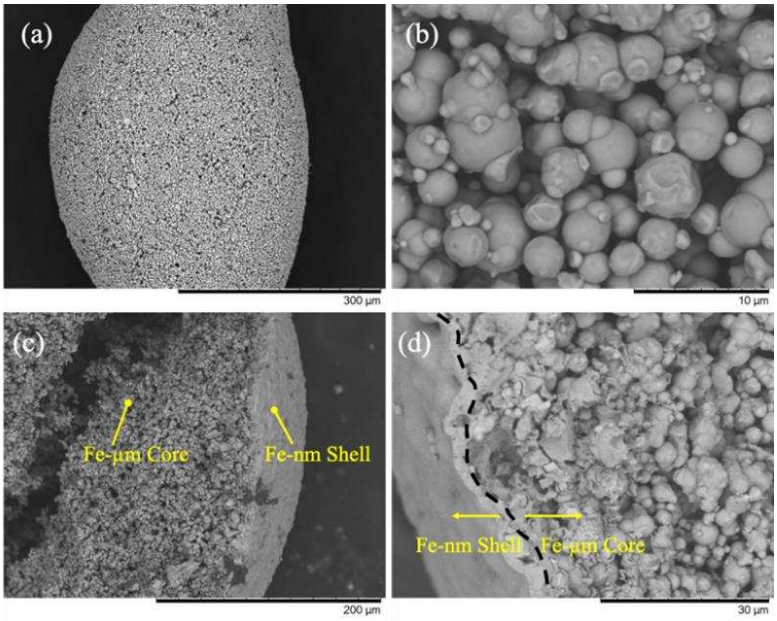

Fig. 7. SEM images of particles agglomerates for (a -b) 30% Fe-µm in diesel fuel and (c-d) 30% hybrid Fe-µm and Fe-nm in diesel fuel.

5. Conclusions

Iron micro- and nanoparticles were investigated as a viable high-energy, carbon-free candidate for combustion systems. Due to their high oxidation rate and reactivity, high concentration colloidal suspensions of iron particles in diesel fuel were considered for a droplet combustion study. 30% concentrations of two types of iron particles, 10 µm, and 40 nm, and their uniform mixture (hybrid) were suspended in diesel fuel without adding surfactant. The major conclusions of this study are as follows:

- The combustion of iron particles in diesel fuel can be characterized by several discernible stages; all three suspensions went through a thermal expansion before ignition, but only in suspensions of nanoparticles in diesel fuel the combustion did follow the d^2-law of combustion with several swelling and puffing events and ended with an isolated event of solid particle combustion. A single intense micro-explosion ended the combustion of microparticles and hybrid particle suspensions.

- The droplet burning rate for suspension of nanoparticles in diesel fuel was found to be similar to that of diesel fuel. While nanoparticles can enhance energy transfer from the flame zone to the droplet, leading to a higher burning rate, their high concentration can suppress the transport of the base fuel to the surface. Yet, the mass loss due to frequent puffing events results in secondary atomization, reducing combustion time overall. As soon as microparticles are added, a strong micro-explosion follows almost immediately after ignition, leading to the complete breakdown of the droplet and dispersion of iron particles into the flame zone. For the hybrid scenario, the microexplosion occurred in a shorter period after ignition and was more intense than the suspensions of microparticles. The intense microexplosion and shortened combustion time offer diesel fuel as both a safe storage environment and also an effective mode for the fast combustion of iron particles.
- Post-evaporation particle agglomerates for suspensions of micro- and hybrid parties were analyzed using SEM microscopy. A comparison between SEM images revealed a thin nanoparticle shell formed around a microparticle after a hybrid droplet's evaporation. The high concentration of nanoparticles near the droplet surface can enhance heat transfer to the droplet, leading to a faster microexplosion. Nanoparticles were also observed to have filled the void spaces between microparticles. As a result, and compared to when only microparticles are present, higher pressure can build up within the droplet, leading to a stronger micro-explosion and fragmentation of the droplet and, ultimately, more efficient combustion of iron particles.

Based on the findings of this study on iron particle combustion in liquid fuels, the following recommendations are suggested:

1. Further research should optimize the ratios and concentrations of micron-sized and nano-sized iron particles in diesel to maximize combustion efficiency and control micro-explosion intensity.
2. Explore the use of different liquid fuels and environmental conditions (e.g., varying oxygen concentrations) to understand their impact on combustion dynamics and particle behavior.
3. Pilot studies in industrial settings, such as furnaces and boilers, should be conducted to validate the feasibility and benefits of using iron-diesel slurries for efficient combustion and nonoxidative storage.

Declaration of competing interest

The authors declare that they have no known competing financial interests or personal relationships that could have appeared to influence the work reported in this paper.

Acknowledgements

This work has been supported by the Saudi Arabia Cultural Bureau in London in a PhD scholarship to AA.

Author Contributions

- A.A.: Investigation, Conceptualization, Data Curation, Formal Analysis, Writing – Original Draft, Visualization
- Y.Z.: Conceptualization, Methodology, Resources, Supervision, Project Administration
- M.G.: Validation, Formal Analysis, Supervision, Writing – Review & Editing

References

[1] J.M. Bergthorson, Recyclable metal fuels for clean and compact zero-carbon power, Progress in Energy and Combustion Science 68 (2018) 169-196.

412 [2] Y. Zhou, J. Liu, D. Liang, W. Shi, W. Yang, J. Zhou, Effect of particle size and
413 oxygen content on ignition and combustion of aluminum particles, Chinese Journal
414 of Aeronautics 30(6) (2017) 1835-1843.
415 [3] J.Z. Zhang, Global patterns of phosphorus transformation in relation to latitude,
416 temperature and precipitation, Pedosphere 31(1) (2021) 214-218.
417 [4] J.M. Bergthorson, Y. Yavor, J. Palecka, W. Georges, M. Soo, J. Vickery, S.
418 Goroshin, D.L. Frost, A.J. Higgins, Metal-water combustion for clean propulsion and
419 power generation, Applied Energy 186 (2017) 13-27.
420 [5] J.M. Bergthorson, S. Goroshin, M.J. Soo, P. Julien, J. Palecka, D.L. Frost, D.J.
421 Jarvis, Direct combustion of recyclable metal fuels for zero-carbon heat and power,
422 Applied Energy 160 (2015) 368-382.
423 [6] N. Rojas-Valencia, J. Gallego, A. Santamaría, Effect of an iron compound added to
424 diesel fuels in both soot reduction capacity and soot oxidation reactivity, Energy &
425 Fuels 31(11) (2017) 12455-12465.
426 [7] S. Zhang, X. Wang, Z. Mao, Y. Li, B. Jin, R. Xiao, Effect of calcination condition
427 on the performance of iron ore in chemical-looping combustion, Fuel Process
428 Technology 203 (2020) 106395.
429 [8] S. Li, J. Huang, W. Wubin, Y. Qian, X. Lu, M. Aldén, Z. Li, Ignition and
430 combustion behavior of single micron-sized iron particle in hot gas flow, Combustion
431 and Flame 241 (2022) 112099.
432 [9] Y. Yao, D. Chang, A. Panahi, Y.A. Levendis, Spectral emissivities and temperatures
433 of burning iron as single particles or groups of particles, Fuel 375 (2024) 132537.
434 [10] D. Ning, Y. Shoshin, J.A. van Oijen, G. Finotello, L.P.H. de Goey, Burn time and
435 combustion regime of laser-ignited single iron particle, Combustion and Flame 230
436 (2021) 111424.

[11] P. Tóth, Y. Ögren, A. Sepman, P. Gren, H. Wiinikka, Combustion behavior of pulverized sponge iron as a recyclable electrofuel, Powder Technology 373 (2020) 210-219.

[12] J. Sun, P. Liu, M. Wang, Molecular dynamics simulations of melting iron nanoparticles with/without defects using a Reaxff reactive force field, Scientific Reports 10 (2020) 3408.

[13] A. Panahi, D. Chang, M. Schiemann, A. Fujinawa, X. Mi, J.M. Bergthorson, Y.A. Levendis, Combustion behavior of single iron particles-part I: an experimental study in a drop-tube furnace under high heating rates and high temperatures, Applied in Energy and Combustion Science 13 (2023) 100097.

[14] J. Wang, Z. Hui, M. Xiao, Research progress of metal fuel motor technology International Journal of Metallurgy and Metal Physics 5 (2020) 056.

[15] A. Gamayel, M.N. Mohammed, S. Al-Zubaidi, E. Yusuf, Advancements in development and characterization of single droplet combustion: A review, Systematics Reviews in Pharmacy 11 (2020) 902-909.

[16] A.M.-D. Faik, Y. Zhang, Multicomponent fuel droplet combustion investigation using magnified high-speed backlighting and shadowgraph imaging, Fuel 221 (2018) 89-109.

[17] A.F. Abdul Rasid, Y. Zhang, Comparison of the burning of a single diesel droplet with volume and surface contamination of soot particles, Proceedings of the Combustion Institute 38(2) (2021) 3159-3166.

[18] A.F. Abdul Rasid, Y. Zhang, Combustion characteristics and liquid-phase visualization of single isolated diesel droplet with surface contaminated by soot particles, Proceedings of the Combustion Institute 37(3) (2019) 3401-3408.

461 [19] P.K. Ojha, R. Maji, S. Karmakar, Effect of crystallinity on droplet regression and
462 disruptive burning characteristics of nanofuel droplets containing amorphous and
463 crystalline boron nanoparticles, Combustion and Flame 188 (2018) 00102180.
464 [20] A. Aboalhamayie, L. Festa, M. Ghamari, Evaporation rate of colloidal droplets of
465 jet fuel and carbon-based nanoparticles: Effect of thermal conductivity,
466 Nanomaterials 9(9) (2019) 1297.
467 [21] Y. Gan, Y.S. Lim, L. Qiao, Combustion of nanofluid fuels with the addition of
468 boron and iron particles at dilute and dense concentrations, Combustion and Flame
469 159(4) (2012) 1732-1740.
470 [22] Y. Gan, L. Qiao, Combustion characteristics of fuel droplets with the addition of
471 nano and micron-sized aluminum particles, Combustion and Flame 158(2) (2011)
472 354-368.
473 [23] S.H. Pourhoseini, M. Ghodrat, M. Baghban, Z. Shams, Effects of blending
474 energetic iron nanoparticles in B20 fuel on lower CO and UHC emissions of the
475 diesel engine in cold start condition, Case Studies in Thermal Engineering 41 (2023)
476 102658.
477 [24] D.H. Napper, Steric stabilization, Journal of Colloid and Interface Science 58(2)
478 (1977) 390-407.
479 [25] Nanostructured & Amorphous Materials, Inc.,
480 https://www.nanoamor.com/inc/sdetail/55340 (accessed November 2023).
481 [26] M.C. Hicks, V. Nayagam, F.A. Williams, Methanol droplet extinction in carbon-
482 dioxide-enriched environments in microgravity, Combustion and Flame 157 (2010)
483 1439–1445.
484 [27] R. Klimek, T. Wright, Spotlight: Image Analysis and Object Tracking Software,
485 2004. https://ntrs.nasa.gov/search.jsp?R=20060011194 (2004, accessed July 2019).

[28] M. Ghamari, A. Ratner, Combustion characteristics of colloidal droplets of jet fuel and carbon-based nanoparticles, Fuel 188 (2017) 182-189.

[29] S. Tanvir, L. Qiao, Droplet burning rate enhancement of ethanol with the addition of graphite nanoparticles: Influence of radiation absorption, Combustion and Flame 44 (2016) 166-34.

[30] S. Tanvir, L. Qiao, Effect of addition of energetic nanoparticles on droplet burning rate of liquid fuels, Journal of Propulsion and Power 31(1) (2014) 408–15.

[31] G. Singh, M. Esmaeilpour, A. Ratner, Investigation of combustion properties and soot deposits of various US crude oils, Energies 12(12) (2019) 2368.

[32] C.K. Law, Recent advances in droplet vaporization and combustion, Progress in Energy and Combustion Science 8(3) (1982) 171-201.

[33] M. Baigmohammadi, W. Prasidha, N.C. Stevens, Y.L. Shoshyn, T. Spee, P. de Goey, Towards utilization of iron powders for heating and power, Applications in Energy and Combustion Science 13 (2023) 100116.